

Inelastic scattering of microwave radiation in the Coulomb blockade: Microwave absorption, amplification, and squeezing by inelastic Cooper-pair tunneling

Juha Leppäkangas^{1,2} and Michael Marthaler^{1,3,4}

¹*Institut für Theoretische Festkörperphysik, Karlsruhe Institute of Technology, 76128 Karlsruhe, Germany*

²*Physikalisches Institut, Karlsruhe Institute of Technology, 76128 Karlsruhe, Germany*

³*Institut für Theorie der Kondensierten Materie,*

Karlsruhe Institute of Technology, 76128 Karlsruhe, Germany

⁴*Theoretische Physik, Universität des Saarlandes, 66123 Saarbrücken, Germany*

We study scattering of propagating microwave fields by a DC-voltage-biased Josephson junction. At sub-gap voltages, a small Josephson junction works merely as a non-linear boundary that can absorb, amplify, and diversely convert propagating microwaves. We find that in the leading-order perturbation theory of the Josephson coupling energy, the spectral density and quadrature fluctuations of scattered thermal and coherent radiation can be described in terms of the well-known $P(E)$ function. Applying this, we show how thermal and coherent radiation can be absorbed and amplified in a circuit with a resonance frequency. We also show when a coherent input can create a two-mode squeezed output. In addition, we evaluate scattering amplitudes between arbitrary photon-number (Fock) states, describing individual photon multiplication and absorption processes occurring at the junction.

I. INTRODUCTION

Charge transport across a mesoscopic constriction is influenced by an interaction with its electromagnetic environment [1–7]. In earlier theoretical studies, the electromagnetic degrees of freedom have usually been traced out from the analysis, with a detailed focus on the mean electric current and its fluctuations. However, recent microwave-circuit experiments have demonstrated a simultaneous measurement of the current as well as various properties of the emitted and scattered microwave fields [8–20]. This technological progress has in turn sparked new theoretical interest to better understand quantum properties of microwave radiation in mesoscopic transport [15, 21–27].

Microwave emission by quantum transport can be a very non-linear interplay. Recent theoretical works predict effects such as photon-emission multistability [28, 29], transmission blockade above certain resonator photon number [30, 31], and photon anti-bunching via charge anti-bunching [21, 32, 33]. Particularly superconducting circuits are interesting in this context, since below the superconducting energy gap, energy released in charge transport is not lost to quasiparticles, but transferred to the electromagnetic degrees of freedom. Here, a Josephson junction has proven to be a versatile tool for engineering non-linear processes with internal driving. It can be used for on-chip production of nonclassical microwaves [19, 25–27, 34, 35], and when interacting with incoming radiation, to realize novel microwave-circuit applications, such as a pump-free parametric amplifier [20].

In this article, we investigate theoretically how different forms of microwave fields scatter by a DC-voltage-biased Josephson junction. We apply an input-output formalism of propagating radiation in a transmission line terminated by a Josephson junction [24]. We show that in the leading-order perturbation theory of the Joseph-

son coupling energy, average spectral properties of scattered thermal and coherent fields can be described in terms of the well-known $P(E)$ function. This function has earlier been used to characterize the average junction current [1, 2] and current fluctuations [8, 20, 24]. In this work, we use it to describe microwave scattering, accounting for an interaction between incoming radiation and junction current fluctuations. We also derive expressions for quadrature fluctuations of the scattered field in terms of the $P(E)$ function. In addition, we show that scattering amplitudes between individual photon-number states (Fock states) are in the perturbative limit determined by quadrature moments of a continuous-mode displacement operator.

Using the derived general formulas, we describe several interesting phenomena they predict. We investigate scattering at low bias voltages and describe an interplay between thermal radiation and Cooper-pair shot noise in an Ohmic transmission line. At higher bias voltages, we study how different types of radiation get absorbed and amplified in a circuit with resonance frequency. Parametric amplification has been demonstrated experimentally in a similar circuit in Ref. [20]. By investigating quadrature fluctuations of the reflected field, we find that an inelastic scattering of a coherent input can create a two-mode squeezed output at specific frequencies. Analogous squeezing effect was recently found also in driven normal-state conductors [11, 36–38]. In the system considered here, it emerges without the presence of quasiparticle excitations. We also show that this two-mode squeezing effect is observable in an Ohmic (broadband) environment and how it becomes enhanced in a resonance circuit. Finally, by applying the treatment based on calculating quadrature moments of a continuous-mode displacement operator, we show that incoming arbitrary photon-number in-states can get converted into arbitrary photon-number out-states. The single-to-multi-photon conversion has been studied recently in Ref. [39] with an

electromagnetic environment consisting of two microwave resonators, in the context of single-photon detection. In this article, we study this effect using a theory that covers more general forms of the electromagnetic environment and arbitrary photon-number inputs, with the restriction to the leading-order perturbation theory in the Josephson coupling energy.

The article is organized as follows. In Sec. II, we introduce the used input-output method that accounts for interaction between microwave radiation and Cooper-pair tunneling in a dc-voltage-biased superconducting transmission line. We introduce the treatment of various microwave fields as the input: thermal radiation, coherent radiation, and single-photon pulses. We also address the connection between incoming coherent radiation and an AC-voltage drive. In Sec. III, we present general formulas describing absorption and conversion of thermal and coherent microwave fields, study in detail an interplay between thermal and shot noise at low bias voltages, and show when absorption and amplification of low- and high-frequency radiation is possible at high bias voltages. In Sec. IV, we study quadrature fluctuations of the output in the case of a coherent input and show when the output can be quadrature squeezed. Finally, in Sec. V, we evaluate scattering-matrix elements between arbitrary photon-number states utilizing a continuous-mode displacement operator. Conclusions and discussion are given in Sec. VI.

II. THE SYSTEM AND THE MODEL

The microwave circuit we consider is shown in Fig. 1. It consists of a DC-voltage-biased superconducting transmission line terminated by a Josephson junction, with coupling energy E_J . In the continuous-mode treatment, the electromagnetic field is described by a semi-infinite lumped-element circuit terminated by the nonlinear Josephson inductance. We consider mostly explicitly an Ohmic transmission line, i.e., a constant inductance L' and capacitance C' per unit length, but the following analysis can be generalized to setups with resonance frequencies [24].

A. Hamiltonian

The starting point of the analysis is the total Hamiltonian [24],

$$H = H_{\text{EE}} + H_J. \quad (1)$$

Here H_{EE} describes the electromagnetic environment, in this case the transmission line including the junction capacitor, and H_J describes Cooper-pair tunneling across the Josephson junction at the end of the transmission line. The combined Hamiltonian of the junction capaci-

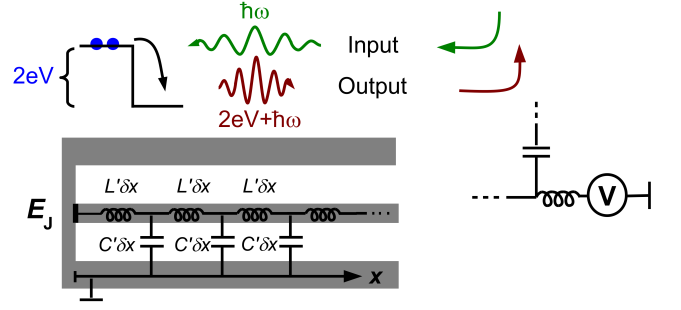


FIG. 1: We study scattering of propagating electromagnetic fields in a semi-infinite transmission line terminated by a Josephson junction. In the dynamical Coulomb blockade regime, a voltage V is applied across the Josephson junction and single-Cooper-pair transport is possible only via emission of a photon at $2eV/\hbar$, or two or more photons at lower frequencies [2, 25]. Incoming radiation of frequency ω can interact with Cooper-pair tunneling and, for example, trigger over-bias emission at $2eV/\hbar + \omega$. In an experimental realization, the Josephson junction can be DC-voltage biased via a low-pass filter as microwave photons propagate and are measured via a high-pass route [8, 19].

tor and of the semi-infinite transmission line has the form

$$H_{\text{EE}} = \frac{\hat{Q}^2}{2C} + \sum_{n=1}^{\infty} \left[\frac{\hat{q}_n^2}{2C'\delta x} + \frac{1}{2L'\delta x} (\hat{\Phi}_n - \hat{\Phi}_{n-1})^2 \right]. \quad (2)$$

This is a sum of inductive (L') and capacitive (C') energies per infinitesimal length δx , enumerated according to nodes (islands) on the central conductor, and added with the charging energy of the junction capacitor (C). The fluxes and charges at each node satisfy $[\hat{\Phi}_n, \hat{q}_m] = 2ie\delta_{mn}$, with $\hat{\Phi}_0$ being the flux and $\hat{Q} = \hat{q}_0$ the charge at the Josephson junction. Other combinations of the commutators are zero. The Cooper-pair tunneling across the Josephson junction is described by the Hamiltonian

$$H_J = -E_J \cos \left(\omega_J t - \frac{2e\hat{\Phi}_0}{\hbar} \right). \quad (3)$$

Here E_J is the Josephson coupling energy and $\omega_J = 2eV/\hbar$ accounts for the DC-voltage bias. In the following we mark $\hat{\phi} \equiv (2e/\hbar)\hat{\Phi}_0$, which corresponds to the superconducting phase difference across the Josephson junction, relative to the applied DC-voltage V .

B. Input-output formulation

In the limit $\delta x \rightarrow 0$, the Heisenberg equations of motion for the magnetic flux at each node convert into a

Klein-Gordon wave equation

$$\ddot{\Phi}(x, t) = \frac{1}{L_i C_i} \frac{\partial^2 \hat{\Phi}(x, t)}{\partial^2 x}. \quad (4)$$

Here $\hat{\Phi}(x, t)$ is the position-dependent magnetic-flux (field) operator. The solution is a propagating electromagnetic field in the transmission line ($x > 0$), which we write in the form

$$\begin{aligned} \hat{\Phi}(x, t) = & \sqrt{\frac{\hbar Z_0}{4\pi}} \int_0^\infty \frac{d\omega}{\sqrt{\omega}} \\ & \times \left[\hat{a}_{\text{in}}(\omega) e^{-i(k_\omega x + \omega t)} + \hat{a}_{\text{out}}(\omega) e^{-i(-k_\omega x + \omega t)} + \text{H.c.} \right]. \end{aligned} \quad (5)$$

The creation operators of the incoming photons, $\hat{a}_{\text{in}}^\dagger(\omega)$, and the corresponding annihilation operators, $\hat{a}_{\text{in}}(\omega)$, follow the commutation relation

$$\left[\hat{a}_{\text{in}}(\omega), \hat{a}_{\text{in}}^\dagger(\omega') \right] = \delta(\omega - \omega'). \quad (6)$$

In a consistent solution, this relation is also valid for the operators of the out-field. This has been shown explicitly to hold at least up to second-order in E_J in Ref. [34]. The wave number has the form $k_\omega = \omega \sqrt{C' L'}$ and the characteristic impedance $Z_0 = \sqrt{L'/C'}$.

At the Josephson junction ($x = 0$) the interaction between the electromagnetic radiation and Cooper-pair tunneling is described by the boundary condition

$$C \ddot{\Phi}(0, t) - \frac{1}{L'} \frac{\partial \hat{\Phi}(x, t)}{\partial x} \Big|_{x=0} = I_c \sin \left[\omega_J t - \hat{\phi}(t) \right]. \quad (7)$$

Here I_c is the junction's critical current, related to the tunneling coupling as $E_J = (\hbar/2e)I_c$. The boundary condition manifests the Kirchhoff's rule for current conservation at the end of the transmission line.

C. Considered input states

In this article, we consider incoming microwave radiation of the following forms: (i) thermal radiation, (ii) stationary coherent radiation with a thermal background, and (iii) a single- or multi-photon pulse.

Let us consider first the treatment of a deterministic coherent signal at frequency ω_0 . At zero temperature such state is constructed as [40]

$$|\text{in}\rangle = \hat{D}|0\rangle \equiv |\alpha\rangle. \quad (8)$$

Here $|0\rangle$ stands for the continuous-mode vacuum and \hat{D} is a displacement operator defined as

$$\hat{D} = \exp \left[\alpha^* \hat{a}_{\text{in}}^\dagger(\omega_0) - \alpha \hat{a}_{\text{in}}(\omega_0) \right]. \quad (9)$$

This satisfies a relation

$$\hat{D}^\dagger \hat{D} = 1. \quad (10)$$

Using the notation $\alpha = \sqrt{2\pi F} e^{i\theta}$, the state gives for the correlation function

$$\langle \hat{a}_{\text{in}}^\dagger(\omega) \hat{a}_{\text{in}}(\omega') \rangle = 2\pi F \delta(\omega - \omega_0) \delta(\omega' - \omega). \quad (11)$$

The photon flux density of the incoming radiation has then the form [40]

$$f_{\text{in}}(\omega) \equiv \frac{1}{2\pi} \int d\omega' \langle \hat{a}_{\text{in}}^\dagger(\omega) \hat{a}_{\text{in}}(\omega') \rangle = F \delta(\omega - \omega_0). \quad (12)$$

The total incoming photon flux is F . Note that in Eq. (11) the delta function $\delta(\omega' - \omega)$ reflects the fact that the photon number of a stationary beam is infinity [40].

We will now account for thermal radiation at lower frequencies. In this article, we assume $\omega_0 \gg k_B T/\hbar$, so that thermal photons do not practically exist at the drive frequency ω_0 . Furthermore, the statistics of thermal radiation is probabilistic, so we need to introduce a (formal) density operator. We then state that the statistics of incoming radiation is described by

$$\hat{\rho} = \hat{D} \hat{\rho}_{\text{th}} \hat{D}^\dagger. \quad (13)$$

Here $\hat{\rho}_{\text{th}}$ describes bare thermal distribution. The relevant quantity in the following being the expectation value

$$\begin{aligned} \langle \hat{a}_{\text{in}}^\dagger(\omega) \hat{a}_{\text{in}}(\omega') \rangle = & \frac{1}{e^{\beta \hbar \omega} - 1} \delta(\omega - \omega') \\ & + 2\pi F \delta(\omega - \omega_0) \delta(\omega' - \omega). \end{aligned} \quad (14)$$

The limit $F = 0$ ($\hat{D} = 1$), then corresponds to the case of a bare thermal input.

In the case of a single-photon input, we can assume a deterministic input state (pulse)

$$|\text{in}\rangle = \hat{a}_\xi^\dagger |0\rangle = \int_0^\infty d\omega \xi(\omega) \hat{a}_{\text{in}}^\dagger(\omega) |0\rangle. \quad (15)$$

Here $\xi(\omega)$ describes the waveform of the incoming photon, with normalization $\int_0^\infty d\omega |\xi(\omega)|^2 = 1$. The finite width is needed, as any finite photon-number field has a form of a pulse [40]. Using Eq. (6) it is then easy to show that such single-photon creation and annihilation operators satisfy

$$[\hat{a}_\xi, \hat{a}_\xi^\dagger] = 1. \quad (16)$$

Multi-photon states are created analogously.

D. Solution as a function of junction current

In the input-output theory, the solution of the out field can be expressed as a function of the time evolution at

the boundary [41]. In our problem, the the out field is then a function of the junction current [24],

$$\begin{aligned} \hat{a}_{\text{out}}(\omega) &= \hat{a}_0(\omega) + i\sqrt{\frac{Z_0}{\pi\hbar\omega}} A(\omega) \int_{-\infty}^{\infty} dt e^{i\omega t} \\ &\times \hat{U}^\dagger(t, -\infty) \hat{I}_J^0(t) \hat{U}(t, -\infty). \end{aligned} \quad (17)$$

Here the zeroth-order scattering state has the form

$$\hat{a}_{\text{out}}(\omega) = \frac{A(\omega)}{A^*(\omega)} \hat{a}_{\text{in}}(\omega) \equiv \hat{a}_0(\omega), \quad (18)$$

where the function $A(\omega)$ accounts for the surrounding linear microwave circuit, for an Ohmic transmission having the form

$$A(\omega) = \frac{1}{1 - i\omega Z_0 C}. \quad (19)$$

This function can also incorporate reflections (resonances) in the transmission line [24]. Therefore, in higher orders, the solution is basically defined by the Fourier transform of the boundary current. A central operator here is the phase difference across the Josephson junction, with the zeroth-order solution ($E_J = 0$) [2, 34]

$$\hat{\phi}_0(t) = \frac{\sqrt{4\pi\hbar Z_0}}{\Phi_0} \int_0^\infty \frac{d\omega}{\sqrt{\omega}} A(\omega) a_{\text{in}}(\omega) e^{-i\omega t} + \text{H.c.} \quad (20)$$

The free-evolution solution ($E_J = 0$) for the junction current is

$$\hat{I}_J^0(t) = I_c \sin[\omega_J t - \hat{\phi}_0(t)], \quad (21)$$

and the time-evolution is defined by the operator [42]

$$\hat{U}(t, t_0) = \mathcal{T} \exp \left\{ \frac{i}{\hbar} \int_{t_0}^t dt' H_J^0(t') \right\}, \quad (22)$$

where \mathcal{T} is the time-ordering operator.

E. Phase-fluctuation function

In the evaluation of the spectral density and quadrature fluctuations of the out-field, a central quantity is the function

$$P(t, t') \equiv \left\langle e^{i\hat{\phi}_0(t)} e^{-i\hat{\phi}_0(t')} \right\rangle. \quad (23)$$

This connects Cooper-pair tunneling to the spectral structure of the electromagnetic environment [1, 2]. The explicit form of this ensemble average depends on the input field. Below we consider the form of this function in the cases of thermal and coherent input.

In thermal equilibrium, the free-evolution phase fluctuations satisfy

tuations satisfy

$$P_{\text{th}}(t, t') = e^{J_{\text{th}}(t-t')}, \quad (24)$$

where the phase-correlation function has the form [2]

$$J_{\text{th}}(t) = \left\langle \left[\hat{\phi}_0(t) - \hat{\phi}_0(0) \right] \hat{\phi}_0(0) \right\rangle_{\text{th}}. \quad (25)$$

Using Eqs. (14) and (20) one obtains

$$\left\langle \hat{\phi}_0(t) \hat{\phi}_0(t') \right\rangle_{\text{th}} = 2 \int_{-\infty}^{\infty} \frac{d\omega}{\omega} \frac{\text{Re}[Z_t(\omega)]}{R_Q} \frac{e^{-i\omega(t-t')}}{1 - e^{-\beta\hbar\omega}}. \quad (26)$$

Here $R_Q = h/4e^2$ is the superconducting resistance quantum and we have defined the (real part of the) tunnel impedance as [2, 24]

$$\text{Re}[Z_t(\omega)] = Z_0 |A(\omega)|^2. \quad (27)$$

Note that the quantity $J_{\text{th}}(t)$ is a complex valued function, accounting for vacuum fluctuations.

To learn how a deterministic high-frequency input state modifies junction phase fluctuations, we rewrite the corresponding ensemble average formally as

$$\left\langle e^{i\hat{\phi}_0(t)} e^{-i\hat{\phi}_0(t')} \right\rangle = \text{Tr} \left\{ \hat{D}^\dagger e^{i\hat{\phi}_0(t)} \hat{D} \hat{D}^\dagger e^{-i\hat{\phi}_0(t')} \hat{D} \rho_{\text{th}} \right\}, \quad (28)$$

where the density operator ρ_{th} describes thermal statistics of the low-frequency radiation and \hat{D} is the (unitary) displacement operator accounting for the high-frequency coherent radiation, see Sec. II C. Consider Taylor expanding the exponential function,

$$\hat{D}^\dagger e^{i\hat{\phi}_0(t)} \hat{D} = 1 + i\hat{D}^\dagger \hat{\phi}_0(t) \hat{D} \quad (29)$$

$$+ \frac{i^2}{2!} \hat{D}^\dagger \hat{\phi}_0(t) \hat{D} \hat{D}^\dagger \hat{\phi}_0(t) \hat{D} + \dots \quad (30)$$

This implies the result

$$\hat{D}^\dagger e^{i\hat{\phi}_0(t)} \hat{D} = e^{i\hat{D}^\dagger \hat{\phi}_0(t) \hat{D}}. \quad (31)$$

For the coherent-state input we use the property [40]

$$\hat{D}^\dagger \hat{a}^{(\dagger)}(\omega) \hat{D} = \hat{a}^{(\dagger)}(\omega) + \alpha^{(*)} \delta(\omega - \omega_0). \quad (32)$$

It follows that incoming coherent radiation can be accounted for by an additional complex number,

$$P_{\text{coh}}(t, t') = e^{i\phi_{\omega_0}(t)} e^{-i\phi_{\omega_0}(t')} e^{J_{\text{th}}(t-t')}, \quad (33)$$

where we have defined

$$\phi_{\omega_0}(t) = \frac{\sqrt{4\pi\hbar Z_0}}{\Phi_0} \frac{A(\omega_0)}{\sqrt{\omega_0}} \alpha e^{-i\omega_0 t} + \text{H.c.} \quad (34)$$

Below, we assume that the additional phase fluctua-

tions due to the incoming coherent signal have the form

$$\phi_{\omega_0}(t) = a \cos \omega_0 t, \quad (35)$$

where a is a real number. Within this choice we have the connection

$$a = \sqrt{\frac{8Z_0}{\omega_0 R_Q}} |\alpha A(\omega)|. \quad (36)$$

Note that the above derivation can be applied for all unitary operators \hat{D} . In particular, it is also valid for continuous-mode squeezed vacuum [40] as input.

F. Treating coherent input as AC-voltage

The specific input state we consider enters the calculation when taking an ensemble average of a studied quantity, such as the junction current or emitted microwave power. A special case is the coherent-state input, where the initial state of the environment can usually be accounted for by an additional complex number. For example, when transforming the free-evolution operator of the junction current by the displacement operator \hat{D} , one gets (see Sec. II E)

$$\hat{I}_J^0(t) \rightarrow \hat{D}^\dagger \hat{I}_J^0(t) \hat{D} = I_c \sin [\omega_J t - \phi_{\omega_0}(t) - \hat{\phi}_0(t)]. \quad (37)$$

Also the time-evolution operator keeps its form in this transformation, following from

$$\hat{H}_J^0(t) \rightarrow \hat{D}^\dagger \hat{H}_J^0(t) \hat{D} = -E_J \cos [\omega_J t - \phi_{\omega_0}(t) - \hat{\phi}_0(t)]. \quad (38)$$

It then follows that in certain situations the incoming coherent radiation can be treated only as an additional AC component of the applied voltage V . More detailed, this approach is valid (at least) when the specific quantities we calculate are defined only by the junction current, i.e., higher-order contributions of the out-field operators, Eq. (17). However, to be able to derive out-field properties at a mode which has also input radiation, the coherent input has to be accounted also by the zeroth-order solution $\hat{a}_0(\omega)$. This can be understood as that here the out-field is a combination of a reflected signal from the junction capacitor and the one emitted (or absorbed) by the junction current. This is the origin for a difference between junction-current power spectrum and output radiation power, investigated more detailed in the next section.

III. SCATTERING OF THERMAL AND COHERENT RADIATION

In this section, we investigate scattering of thermal and coherent microwave radiation by a DC-voltage biased

Josephson junction. We start by presenting general formulas for the photon flux density and power spectral density, describing changes between the incoming and outgoing microwave fields at certain frequency. After this, we analyze more detailed specific phenomena predicted by these formulas, namely conversion and absorption of thermal radiation at low-frequencies and amplification of coherent signals at high frequencies. Quadrature fluctuations (and quadrature squeezing) of the outgoing field will be studied in Sec. IV. Simultaneous dispersive shift in the reflected field has been investigated recently experimentally in Ref. [15] and the absorption and amplification in the drive mode in Ref. [20].

A. General formulas

Here, we introduce our expressions that describe changes in the photon flux and power density between the incoming and outgoing fields. Our results are obtained by a leading-order expansion in the Josephson energy E_J , presented more detailed in Appendix A. The technical calculation involves time integrations of quantities similar to phase-fluctuation function $P(t, t')$, Eq. (23).

The photon flux density of propagating fields in the transmission line is generally defined as [40]

$$f_{\text{in/out}}(\omega) \equiv \frac{1}{2\pi} \int d\omega' \langle \hat{a}_{\text{in/out}}^\dagger(\omega') \hat{a}_{\text{in/out}}(\omega) \rangle, \quad (39)$$

and the equivalent power density accounts for the single-photon energy $\hbar\omega$ and is then

$$\mathcal{P}_{\text{in/out}}(\omega) = \hbar\omega f_{\text{in/out}}(\omega). \quad (40)$$

In the following, we present the total result using different contributions in the form

$$f_{\text{out}}(\omega) - f_{\text{in}}(\omega) = f_{\text{em}}(\omega) - f_{\text{abs}}(\omega). \quad (41)$$

The left-hand side then considers the difference between incoming and outgoing photon fluxes (or powers) and the right-hand side contributions can be interpreted as inelastic processes where new radiation is created (em) and incoming radiation is absorbed (abs). The identification of these terms is based on having similar forms of the probability distribution $P(E)$. However, only the sum $f_{\text{em}}(\omega) - f_{\text{abs}}(\omega)$ should be considered as a physical result, due to divergence of certain terms at $\omega = 0$. The term $f_{\text{in}}(\omega)$ corresponds to the result for $E_J = 0$ and is determined by Eq. (14). By our definition, all individual components of the photon flux density are positive.

1. Emission and absorption

The function $f_{\text{em}}(\omega) \geq 0$ describes how radiation will be emitted by the junction current fluctuations. The con-

tribution can be expressed as

$$f_{\text{em}}(\omega) = \frac{1}{1 - e^{-\beta\hbar\omega}} \frac{I_c^2 \text{Re}[Z_t(\omega)]}{2\omega} \quad (42)$$

$$\times \sum_{\pm} \sum_{n=-\infty}^{\infty} P[\hbar(\pm\omega_J - n\omega_0 - \omega)] |J_n(a)|^2$$

$$+ \delta(\omega - \omega_0) \frac{I_c^2 R_Q}{4} \sum_{\pm} \sum_{n=1}^{\infty} |J_n(a)|^2 n P[\hbar(\pm\omega_J - n\omega_0)] .$$

This is a function of the well-known probability distribution $P(E)$ [1, 2], defined as the Fourier transform of the phase correlation function of the thermal field, Eq. (24),

$$P(E) = \frac{1}{2\pi\hbar} \int_{-\infty}^{\infty} dt \left\langle e^{i\hat{\phi}_0(t)} e^{-i\hat{\phi}_0(0)} \right\rangle_{\text{th}} e^{i\frac{E}{\hbar}t}$$

$$= \frac{1}{2\pi\hbar} \int_{-\infty}^{\infty} dt e^{J_{\text{th}}(t) + i\frac{E}{\hbar}t} , \quad (43)$$

Here, the plus (minus) sign in front of ω_J corresponds to contribution from forward (backward) Cooper-pair tunneling. Since the result for bare thermal radiation corresponds to $a = 0$, we see that for a finite amplitude a , sidebands appear to the emission spectrum, separated by multiples of the drive frequency ω_0 . The summation over n then corresponds to a number of photons exchanged with the drive field in a tunneling process. Positive (negative) value means emission into (absorption from) the drive frequency. The extra contribution at frequency ω_0 [the bottom line of Eq. (42)] then describes the effect of such emission to the drive mode. We note that the imaginary part of Eq. (43), appearing if the time integration would be done only from zero to infinity, is related to a phase shift of the reflected radiation [15] as well as to energy shifts (instead of transition rates) in analogous master-equation approaches [43].

The result for the function $f_{\text{abs}}(\omega) \geq 0$ is analogous. It describes how radiation is absorbed by the junction current fluctuations and has the form

$$f_{\text{abs}}(\omega) = \frac{1}{e^{\beta\hbar\omega} - 1} \frac{I_c^2 \text{Re}[Z_t(\omega)]}{2\omega} \quad (44)$$

$$\times \sum_{\pm} \sum_{n=-\infty}^{\infty} P[\hbar(\pm\omega_J - n\omega_0 + \omega)] |J_n(a)|^2$$

$$+ \delta(\omega - \omega_0) \frac{I_c^2 R_Q}{4} \sum_{\pm} \sum_{n=1}^{\infty} |J_n(a)|^2 n P[\hbar(\pm\omega_J + n\omega_0)] .$$

Here, again, the plus (minus) sign in front of ω_J corresponds to contribution from forward (backward) Cooper-pair tunneling and the summation over n then corresponds to a number of photons exchanged with the drive field in a tunneling process. The extra contribution at frequency ω_0 [the last contribution on the right-hand side of Eq. (44)] describes the effect of such absorption to the drive mode. Note that the front factor of the first contribution on the right-hand side decays exponentially

to zero with temperature, unlike the corresponding term in emission, Eq. (42). The functions f_{em} and f_{abs} are related by the transformation $\omega \rightarrow -\omega$ and $n \rightarrow -n$, reflecting that emission and absorption are in a quantum theory connected by a sign change in the Fourier transformation of a noise correlation function.

2. Junction current fluctuations

In earlier works, a direct connection between the $P(E)$ theory and junction current fluctuations has been established [8, 20, 24, 25]

$$\left\langle \hat{I}_J(t) \hat{I}_J(0) \right\rangle_{\omega} \quad (45)$$

$$= \pi\hbar \frac{I_c^2}{2} \sum_{\pm} \sum_{n=-\infty}^{\infty} P[\hbar(\pm\omega_J - n\omega_0 - \omega)] |J_n(a)|^2 ,$$

This differs from f_{em} by not having $(1 - e^{-\beta\hbar\omega})^{-1}$ and $\text{Re}[Z_t(\omega)]$ as front factors. In the zero-temperature limit, the power density of the emitted radiation is then, up to a frequency-dependent front factor, the finite-frequency current noise of the Josephson current [24]. At finite temperatures, however, this is not the total spectrum of out-radiation, since the formula based only on the current fluctuations does not correctly account for changes in the input field. This becomes evident, for example, when looking the contribution at coherent drive frequencies (delta-function contributions), which are missing in the current correlator. In an exactly similar way, the absorption of (and the induced emission to) the thermal field is not included. This difference to the current-current correlator is studied further below.

B. Low-frequency phenomena

We study now how the current-current correlator spectrum and the out-field spectrum differ in the case of a low-Ohmic environment. We also investigate how they differ for a circuit with a resonance frequency in the neighborhood of resonance condition for a photon emission in the resonance mode.

1. Disappearance of the junction at $V = 0$

An illustrative example of changes between incoming and outgoing fields is the case of zero voltage bias, $V = 0$, and the absence of coherent drive, $a = 0$. Here, the power supplied by the voltage source vanishes, $IV = 0$, so no changes in the total power is expected (the energy conservation for general V is shown in Appendix B). We can then use the detailed balance symmetry of the $P(E)$

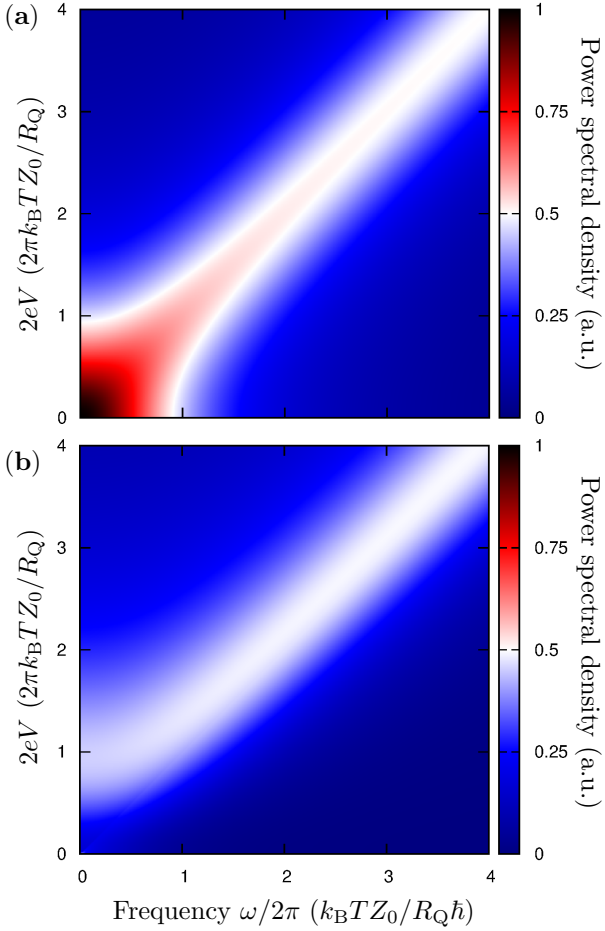


FIG. 2: (a) The power spectral density of Josephson-junction current fluctuations, $\langle \hat{I}_J(t) \hat{I}_J(0) \rangle_\omega$, for a voltage V biased Ohmic transmission line and a thermal input. The current fluctuations occur predominantly at the diagonal line, corresponding to the Josephson radiation frequency, $\omega = 2eV/\hbar$. (b) The simultaneous change in the power density, $\mathcal{P}_{\text{out}}(\omega) - \mathcal{P}_{\text{in}}(\omega)$. The 'bending' and disappearance of the added power at $2eV/\hbar = 0$ manifests that at zero bias the Josephson junction does not change the spectrum of the propagating thermal field at all. For a finite voltage bias, however, a maximum of added zero-frequency noise occurs near $2eV = 2\pi k_B T Z_0 / R_Q$. We consider here a transmission-line characteristic impedance $Z_0 = 100 \, \Omega$, a junction capacitance $C_J = 100 \, \text{fF}$, and a temperature $T = 100 \, \text{mK}$.

function [2], $P(-E) = e^{-\beta E} P(E)$, to show that

$$f_{\text{em}}(\omega) - f_{\text{abs}}(\omega) = 0. \quad (46)$$

Thus, an undriven and unbiased Josephson junction does not modify the thermal radiation at all: The outgoing radiation is still thermal and exactly of the same form as the input radiation. This result is seen in Fig. 2(b), as the 'avoided crossing' emerging at $2eV/\hbar = 0$, in comparison to the diagonal Josephson AC-current line (in current fluctuations) in Fig. 2(a).

For higher DC voltages, however, an additional zero-

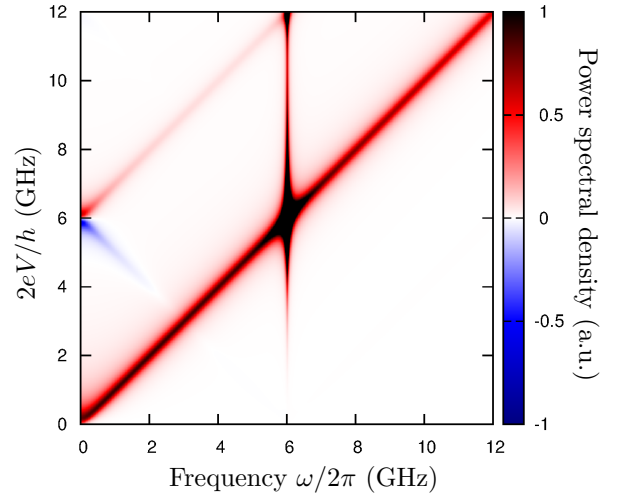


FIG. 3: The added power, $\mathcal{P}_{\text{out}}(\omega) - \mathcal{P}_{\text{in}}(\omega)$, by a voltage V biased Josephson junction in a transmission line with a resonance frequency at $\omega_r/2\pi = 6 \, \text{GHz}$ and in the case of incoming thermal radiation ($a = 0$). Emission at the Josephson frequency (the diagonal line) is enhanced close to the resonance frequency $2eV/\hbar = \omega_r$. In particular, when biased just below the resonance frequency, $2eV/\hbar \lesssim \omega_r$, emission to the resonance frequency absorbs incoming thermal radiation (blue region at low frequencies). Vice versa, when biased just above the resonance frequency. The parameters are $Z_0 = 100 \, \Omega$, $C_J = 100 \, \text{fF}$, $T = 100 \, \text{mK}$, and we have also added an additional term in the impedance $\text{Re}[Z_t(\omega)]$, corresponding to an impedance of a $\omega_r/2\pi = 6 \, \text{GHz}$ resonator with quality factor 100 and characteristic impedance $Z_{LC} = 100 \, \Omega$.

frequency noise appears. For low-Ohmic environments, the noise has a maximum approximately at $2eV = 2\pi k_B T R / R_Q$, as seen Fig. 2(b). This value corresponds to the width of the current-fluctuation spectrum around $\hbar\omega = 2eV$ at all voltages [24]. At higher voltage-biases, the change in the power spectrum approaches the spectrum of the current correlator. More detailed, the additional out spectrum becomes a sum of a term proportional to $\langle I_J(t) I_J(0) \rangle_\omega$ and a term

$$\frac{1}{e^{\beta \hbar \omega} - 1} \frac{\hbar I_c^2 \text{Re}[Z_t(\omega)]}{2} \times [P(2eV - \hbar\omega) - P(2eV + \hbar\omega)]. \quad (47)$$

Thus, in the limit $\omega \rightarrow 0$, this additional contribution becomes proportional to $k_B T \partial P(E) / \partial E|_{E=2eV}$. This is then compared to $P(2eV)$, the magnitude of $\langle I_J(t) I_J(0) \rangle_{\omega=0}$. For a low-Ohmic transmission line, and in the limit $E \gg k_B T$, we have $P(E) \sim Z_0 / R_Q E$. This means that for $k_B T / 2eV < 1$ the correction to the low-frequency noise is dominated by the shot noise in the junction current, as also seen in Fig. 2(a-b) (the similarity of the two spectral densities at high bias voltages). The interplay between shot noise and thermal fluctuations in the power spectrum has been analyzed recently also in Ref. [44].

2. Low-frequency absorption in a resonance circuit

Absorption of radiation occurs when the contribution $f_{\text{out}}(\omega) - f_{\text{in}}(\omega)$ is negative. Such a result is sound as long as the total flux, $f_{\text{out}}(\omega) = f_{\text{in}}(\omega) + f_{\text{em}}(\omega) + f_{\text{abs}}(\omega)$, is positive. In this case, incoming radiation is extracted from certain frequencies and emitted to other frequencies.

Such an effect occurs in a circuit with resonance frequency $\omega_r \gg k_B T/\hbar$, when voltage biased just below the single-photon emission resonance $\omega_J \lesssim \omega_r$. Here, thermal-photon assisted Cooper-pair tunneling, with emission to the resonance frequency, is favored. We obtain that absorption occurs if

$$P(2eV - \hbar\omega) + \frac{1}{e^{\beta\hbar\omega} - 1} [P(2eV - \hbar\omega) - P(2eV + \hbar\omega)] < 0. \quad (48)$$

Note that this condition includes only $P(E)$ functions, in addition to the Bose factor $1/(e^{\beta\hbar\omega} - 1)$. Multiplying this expression by $\hbar I_c^2 \text{Re}[Z_t(\omega)]/2$ one then obtains the absorption power density. Here, the interpretation is that Cooper-pair tunneling extracts thermal radiation as described by the term $P(2eV + \hbar\omega)$, emits new radiation induced by thermal radiation field, the middle term $P(2eV - \hbar\omega)$, and emits new radiation induced by vacuum fluctuations, the first term $P(2eV - \hbar\omega)$. The cooling effect is seen as the blue region in Fig. 3. This effect naturally works also vice versa: Biasing just above heats the environment. Here, in both cases, the process occurs with a single-photon emission to the resonance frequency ω_r , and is in this sense of parametric type.

C. Drive field amplification

We discuss here briefly the amplification and absorption at the drive frequency. An experimental demonstration and detailed analysis of a similar effect is given in Ref. [20]. This effect can occur even for a simple Ohmic transmission line, but is enhanced in the case of a resonance circuit. Here, the changes in the outgoing single mode flux at ω_0 is characterized by

$$G \equiv \frac{f_{\text{out}}(\omega_0)}{f_{\text{in}}(\omega_0)} = \frac{4\pi I_c^2 \text{Re}[Z_t(\omega_0)]}{\omega_0} \times \frac{\sum_{\pm} \sum_{n=-\infty}^{\infty} |J_n(a)|^2 n P[\hbar(\pm\omega_J - n\omega_0)]}{a^2}, \quad (49)$$

where we have assumed an incoming coherent state $|\alpha\rangle$, whose flux is $|\alpha|^2/2\pi$ and found the equivalent parameter a by using the connection Eq. (36). We then consider flux changes in the delta-function contributions in Eqs. (42) and (44).

Consider now a circuit with resonance frequency $\omega_r = \omega_0$. Two competing effect exists when $\omega_J \approx \omega_r$. When tuned slightly above the resonance condition, $\omega_J \gtrsim \omega_r$, induced emission to the drive frequency occurs through for-

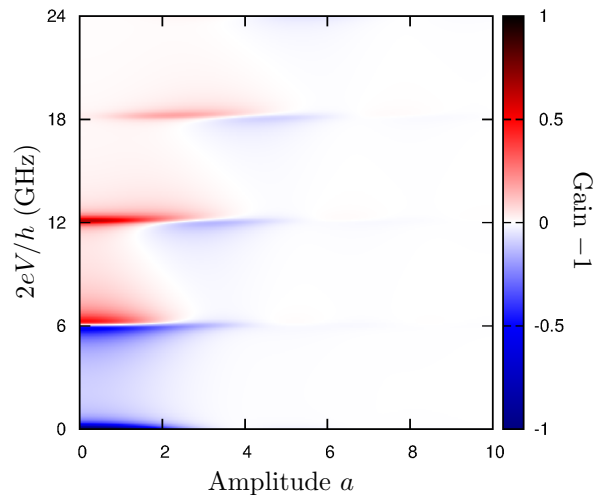


FIG. 4: The gain $G - 1$ of drive field, as defined by Eq. (49), for different drive amplitudes a and bias voltages V . We consider a coherent signal at $\omega_0/2\pi = 6$ GHz and a system as in Fig. 3. Depending on the voltage bias, Cooper-pair tunneling can increase or decrease the flux of photons at ω_0 . In particular, just above $2eV/\hbar = \omega_0$ (and $a \lesssim 2$), induced emission to the drive beam occurs through forward Cooper-pair tunneling and low-frequency photon emission. Just below $2eV/\hbar = \omega_0$, photons are absorbed from the drive beam through backward Cooper-pair tunneling and (again) low-frequency photon emission. The value of $G - 1$ is normalized here by $0.02\pi I_c^2 \text{Re}[Z(\omega_0)]/\hbar\omega_0 \text{GHz}$.

ward Cooper-pair tunneling and additional low-frequency photon emission. Just below the resonance condition, absorption of photons from the drive occurs through backward Cooper-pair tunneling with again low-frequency photon emission. At the exact resonance, these two processes cancel each other. The width and strength of this effect depend on temperature, but we find that the amplification is most prominent at zero temperature, meaning that presence of thermal photons are indeed not needed for amplification. Similar processes are present also for multiphoton resonances $\omega_J \approx n\omega_r$. Numerical results for G as a function of amplitude a and bias voltage are plotted in Fig. 4. The effect is analogous to parametric amplification, with signal-photon induced parametric down conversion to the signal frequency and to the low-frequency environment, the Josephson frequency $2eV/\hbar$ playing the role of the pump field. In Ref. [20], with a two-resonator setup, this effect has been used to realize a pump-field free parametric amplifier.

D. Validity region of the perturbative approach

In this article, we restrict to a leading-order perturbation theory in powers of the Josephson coupling energy E_J [or equivalently the critical current $I_c = (2e/\hbar)E_J$]. We then implicitly assume the limit of weak interaction, where most of the input radiation is reflected, and this

zeroth-order solution dominates when compared to the higher-order contributions. A nonperturbative treatment in E_J in a setup consisting of two microwave resonators has been presented in Ref. [39]. A perturbative calculation of coherence functions beyond the leading order in E_J is on the other hand presented in Ref. [24].

IV. COHERENT INPUT: QUADRATURE SQUEEZED OUTPUT

Microwave radiation can scatter inelastically at a DC-voltage biased Josephson junction. In this section, we investigate quadrature fluctuations of the created output in such processes. An electromagnetic field with quadrature fluctuations less than vacuum fluctuations is called quadrature squeezed and has numerous applications in quantum information and metrology [45]. Quadrature squeezed states are also an optical analog of EPR (Einstein-Podolsky-Rosen) states of two momentum-entangled particles [45].

A. Connection to previous works

Quadrature squeezed microwave radiation can be created in transmission lines with second-order nonlinearities, for example, provided by Josephson junctions [46–51]. They can also be emitted by quantum transport. For example, inelastic Cooper-pair tunneling produces nonclassical photon pairs below the classical Josephson radiation peak, when DC-voltage biased at $V \gg k_B T/2e$ [19, 25, 35], and this radiation is ideally also quadrature squeezed [26]. However, as being sensitive to junction phase fluctuations, such squeezing (with respect to a fixed angle) is washed out in a dephasing time that is in typical experimental conditions less than a microsecond [34]. Here, we describe creation of photon pairs and quadrature squeezing in a different process. Opposed to the case of photon-pair production from a single Cooper-pair tunneling event, Fig. 5(a), this process includes two opposite-direction Cooper-pair tunneling events and absorption of one drive photon, Fig. 5(b). Such production is thereby robust against low-frequency voltage fluctuations, since the total energy of the two photons does not depend on the bias voltage. An analogous phenomenon has been recently predicted [36–38] and measured [11] for normal-state conductors.

B. Definition of squeezing for continuous-mode fields

We start the analysis from the definition of quadrature squeezing for continuous-mode fields [40]. When photons are created only in pairs, the quantum fluctuations of the field quadratures can increase or decrease with respect to vacuum fluctuations. To illustrate this, we first study

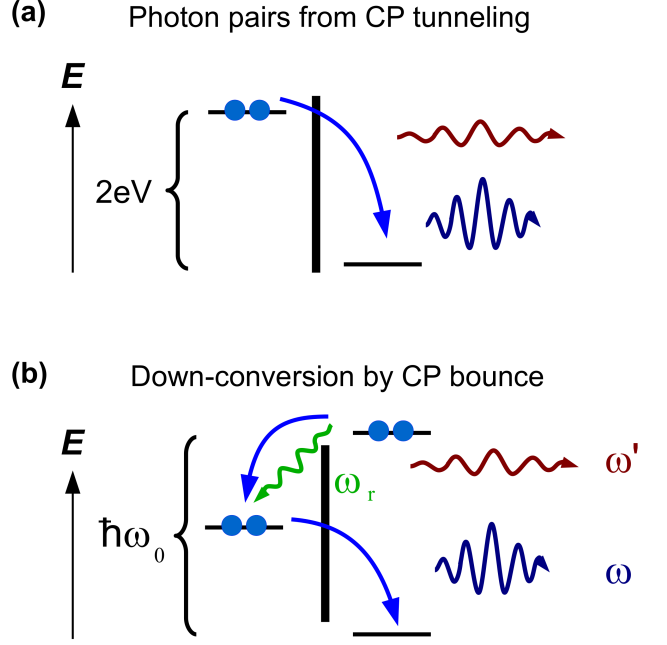


FIG. 5: Two different ways to produce nonclassical photon pairs and quadrature squeezing by a DC-voltage biased Josephson junction. In case (a), two photons are created from the electrostatic energy released in a single Cooper-pair (CP) tunneling event. The process is similar to a parametric down conversion of a pump field at frequency $\omega_J = 2eV/\hbar$. In case (b), correlated drive-photon assisted forward and backward CP tunneling events produce in total two outgoing photons, whose frequencies sum up to the drive frequency ω_0 . In between a virtual photon of frequency ω_r is exchanged. Only process (b) is robust against low-frequency voltage fluctuations, since the total energy of the two outgoing photons does not depend on the (fluctuating) junction voltage. A drive-photon assisted single CP tunneling would be equivalent to process (a) and thereby affected by low-frequency fluctuations.

fluctuations of a field operator

$$\hat{O} = \int_{\text{BW}} d\omega \left[\hat{a}(\omega) e^{-i\theta(\omega)} + \hat{a}^\dagger(\omega) e^{+i\theta(\omega)} \right]. \quad (50)$$

Here BW stands for the detector bandwidth, in general introducing a detector filter function [24, 52], in the simplest case just implying integration between two frequencies. The variable $\theta(\omega)$ corresponds to a continuous-mode generalization of the considered quadrature angle. Fluctuations of this field are then characterized by the variance

$$\text{Var}[\hat{O}] \equiv \left\langle \left(\hat{O} - \langle \hat{O} \rangle \right)^2 \right\rangle = \langle \hat{O}^2 \rangle - \langle \hat{O} \rangle^2, \quad (51)$$

which can be written as

$$\text{Var}[\hat{O}] = \int_{\text{BW}} d\omega \int_{\text{BW}} d\omega' O(\omega, \omega'), \quad (52)$$

where

$$O(\omega, \omega') = \delta(\omega - \omega') + 2 \langle \hat{a}_1^\dagger(\omega) \hat{a}_1(\omega') \rangle + 2 \operatorname{Re} \left[\langle \hat{a}_1(\omega) \hat{a}_1(\omega') \rangle e^{2i\theta(\omega)} \right]. \quad (53)$$

The first term on the right-hand side of Eq. (53) is the result for the vacuum, whose total contribution we mark now as

$$\operatorname{Var}[\hat{O}]_{\text{vac}} = \int_{\text{BW}} d\omega. \quad (54)$$

This is also the minimum uncertainty of a classical field.

We consider first a squeezed state $\hat{D}_{\text{sq}}|0\rangle$, where the continuous-mode squeezing operator is defined as [40]

$$\hat{D}_{\text{sq}} = e^{\hat{P} - \hat{P}^\dagger} \quad (55)$$

$$\hat{P}^\dagger = \frac{1}{2} \int_0^{\omega_0} d\omega \beta(\omega) \hat{a}^\dagger(\omega) \hat{a}^\dagger(\omega_0 - \omega). \quad (56)$$

Here $\beta(\omega) = s(\omega)e^{iv(\omega)}$, with $s(\omega) > 0$, accounts for the frequency distribution of the radiation. By definition, it satisfies $\beta(\omega_0 - \omega) = \beta(\omega)$. This creates photon pair states symmetrically around the central frequency $\omega_0/2$. This type of radiation is created, for example, in a parametric down-conversion [40]. The corresponding photon flux density is

$$\langle \hat{a}^\dagger(\omega) \hat{a}(\omega') \rangle = \sinh^2[s(\omega)] \delta(\omega' - \omega). \quad (57)$$

The key property of a quadrature squeezed field is a finite value of the "nondiagonal" correlator

$$\langle \hat{a}(\omega) \hat{a}(\omega') \rangle = \cosh[s(\omega)] \sinh[s(\omega')] e^{iv(\omega')} \times \delta(\omega + \omega' - \omega_0). \quad (58)$$

This leads to the variance

$$\begin{aligned} \operatorname{Var}[\hat{O}] &= \operatorname{Var}[\hat{O}]_{\text{vac}} + 2 \int_{\text{BW}} d\omega \sinh^2[s(\omega)] \\ &+ 2 \int_{\text{BW}} d\omega \cosh[s(\omega)] \sinh[s(\omega)] \cos[\theta(\omega) - v(\omega)]. \end{aligned} \quad (59)$$

Particularly, the choices $\theta(\omega) = v(\omega)$ and $\theta(\omega) = v(\omega) + \pi$ give the maximal and minimal variances, respectively,

$$\operatorname{Var}[\hat{O}] = \operatorname{Var}[\hat{O}]_{\text{vac}} + \int_{\text{BW}} d\omega \{ \exp[\pm s(\omega)] - 1 \} \quad (60)$$

where the plus (minus) sign corresponds to the maximum (minimum). Thus, for $s(\omega) \rightarrow \infty$ and $\theta(\omega) = v(\omega) + \pi$, the total variance approaches zero and the state becomes perfectly squeezed (with respect to the chosen angle).

C. Quadrature squeezing in the dynamical Coulomb blockade

Let us repeat the analysis of Sec. IV B but now using the solution we obtained for the scattered field in Eq. (17). We study fluctuations of the (outgoing) transmission-line voltage

$$\hat{V} = V_0 \int_{\text{BW}} d\omega \left[\sqrt{\omega} \hat{a}_{\text{out}}(\omega) e^{-i\theta(\omega)} + \sqrt{\omega} \hat{a}_{\text{out}}^\dagger(\omega) e^{+i\theta(\omega)} \right] \quad (61)$$

where $V_0 = \sqrt{\hbar Z_0/4\pi}$. The vacuum fluctuations are here then characterized by a variance

$$\operatorname{Var}[\hat{V}]_{\text{vac}} = V_0^2 \int_{\text{BW}} \omega d\omega. \quad (62)$$

Important is the magnitude of the diagonal correlator of type $\langle \hat{a}_{\text{out}}^\dagger(\omega) \hat{a}_{\text{out}}(\omega') \rangle$, defined by the photon flux density. In the leading-order perturbation theory in powers of E_J , this has the form

$$\begin{aligned} \omega \langle \hat{a}_{\text{out}}^\dagger(\omega) \hat{a}_{\text{out}}(\omega') \rangle &= \pi \delta(\omega - \omega') \\ &\times \sum_{n\pm} |J_n(a)|^2 I_c^2 Z_0 |A(\omega)|^2 P[\hbar(\pm\omega_J - n\omega_0 - \omega)]. \end{aligned} \quad (63)$$

We assume here $\omega, \omega' \gg k_B T/\hbar$ and $\omega, \omega' \neq \omega_0$. Essential is a finite value of the "nondiagonal" correlator $\langle \hat{a}_{\text{out}}(\omega) \hat{a}_{\text{out}}(\omega') \rangle$, which is possible when having a coherent input. We get (Appendix C)

$$\begin{aligned} \sqrt{\omega\omega'} \langle \hat{a}_{\text{out}}(\omega) \hat{a}_{\text{out}}(\omega') \rangle &= \pi I_c^2 Z_0 A(\omega) A(\omega') \\ &\times \sum_{n\pm} \pm i P[\hbar(\omega \mp \omega_J + n\omega_0)] J_n(a) J_{n+1}(a) \delta(\omega + \omega' - \omega_0). \end{aligned} \quad (64)$$

We consider here contributions with mode frequencies that sum to ω_0 . Unlike the photon flux density, this term can also be negative.

Using the simplified notation

$$\sqrt{Z(\omega)} \equiv \sqrt{Z_0 |A(\omega)|^2}, \quad (65)$$

we get a final result for the variance defined in Eq. (51),

$$\begin{aligned} \operatorname{Var}[\hat{V}] - \operatorname{Var}[\hat{V}]_{\text{vac}} &= I_c^2 V_0^2 \int_{\text{BW}} d\omega \\ &\times \left[\sum_{n\pm} |J_n(a)|^2 Z(\omega) P[\hbar(\pm\omega_J + n\omega_0 - \omega)] + m \sum_{n\pm} J_n(a) J_{n+1}(a) \sqrt{Z(\omega)} \sqrt{Z(\omega_0 - \omega)} \{ \pm P[\hbar(\pm\omega_J + n\omega_0 + \omega)] \} \right]. \end{aligned} \quad (66)$$

We assume here that the integration range includes frequencies symmetrically around $\omega_0/2$. In the following, we call the integrand of this expression as the quadrature fluctuation density. The left-hand side of Eq. (66) then compares the fluctuations of the out field to vacuum fluctuations. On the right-hand side we consider only the maximum values of the variance (as a function of squeezing angle θ), which leads to that the introduced variable m is either -1 or 1 (both of them can correspond to the minimum). We then find that in the leading-order perturbation theory also the quadrature fluctuations can be described in terms of the $P(E)$ -function and environmental impedance.

The quadrature fluctuation density (with respect to vacuum) is visualized in Fig. 6(a) for an Ohmic transmission line and in Fig. 6(b) for a circuit with a resonance frequency. We plot here the integrand of Eq. (66) as a function of emission frequency ω and voltage V , when summed over the values at ω and $\omega' = \omega_0 - \omega$ (integration range is assumed to be symmetric around $\omega_0/2$). We find that for an Ohmic environment weak squeezing can occur for $\omega, \omega' \gtrsim 2eV/\hbar$, in a broadband region where the emission from forward Cooper-pair tunneling is minimized. For a resonance frequency at ω_r , on the other hand, we find that two-mode squeezing is strongly enhanced at a line $\hbar\omega = 2eV + \hbar\omega_r$ or equivalently at $\hbar(\omega_0 - \omega') = 2eV + \hbar\omega_r$, see Fig. 6(b). The interpretation is that at this line two-photon emission to frequencies ω' and ω_r occurs via drive-photon assisted backward tunneling, since now $\hbar(\omega' + \omega_r) = \hbar\omega_0 - 2eV$. This line also corresponds to the forward-tunneling process, where a photon from the resonator is absorbed to create a photon to frequency $\omega = 2eV/\hbar + \omega_r$. This combination of processes is visualized in Fig. 5(b). Another squeezing line we see in Fig. 6(b) is $\hbar\omega = -2eV + \hbar\omega_r$ or equivalently $\hbar(\omega_0 - \omega') = -2eV + \hbar\omega_r$. This correspond to the same processes as described above, but with reverse Cooper-pair tunneling directions. Note that squeezing does not occur at $\omega = \omega_r$.

In comparison to other works, we then find that the oscillator state at frequency ω_r plays the same role as virtual population of quasiparticle states in the analogous effect in normal-state systems [11, 36–38]. Also in our system, no squeezing appears when $V = 0$. However, in a very similar setup, quadrature squeezing has been studied and measured in the framework of dynamical Casimir effect [46, 47, 50, 51]. Here, one has $V = 0$ but a large Josephson coupling energy E_J . In this situation, squeezing of the out field can indeed appear in long-time averages since the down-converted pairs have a fixed relative phase, provided by the “trapping” of the phase to a local minimum of the Josephson potential energy, $-E_J \cos \hat{\phi}$. This effect then occurs in the limit of large E_J . The physics is equivalent to a parametric down-conversion of the drive field [40, 45].

It should be emphasized that the size of squeezing our perturbation theory can model is of course limited. Obviously, the critical current cannot be too large for the

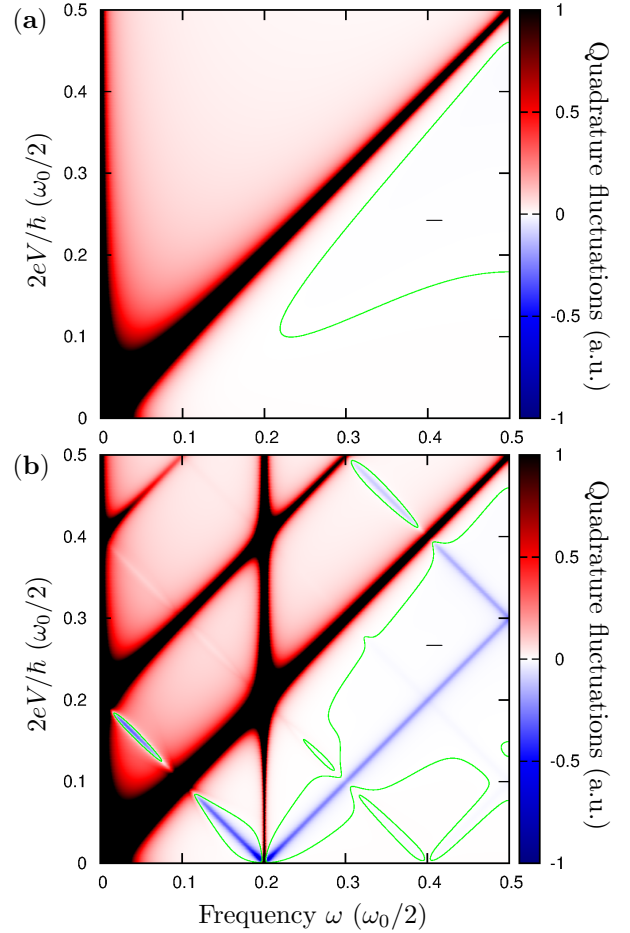


FIG. 6: The quadrature fluctuations with respect to vacuum fluctuations between frequencies ω and $\omega' = \omega_0 - \omega$ of a coherently driven voltage V biased Josephson junction. We plot here the integrand of Eq. (66), when summed over frequencies ω and ω' . The coherent drive at ω_0 has an amplitude $a = 0.75$. (a) For an Ohmic transmission line, the variance can go below the vacuum level when $\omega, \omega' \gtrsim 2eV/\hbar$, where direct emission of photons from the voltage V is prohibited. This broadband region is indicated by the $-$ sign inside the contour line for vacuum fluctuations. (b) For a transmission line with a resonance frequency at $\omega_r = 0.2\omega_0$, two-mode squeezing occurs in the same region as for the Ohmic case, as well as in several other islands, surrounded by the vacuum fluctuation contour lines. Strong squeezing occurs at resonance lines corresponding to processes visualized in Fig. 5(b). The parameters are as in Fig. 3, but with $\omega_0/2\pi = 10$ GHz, $\omega_r/2\pi = 2$ GHz, $Z_{LC} = 700 \Omega$, and $T = 20$ mK.

perturbation theory to hold, otherwise taking the total variance to negative values. Basically, the assumption made here is that the phase noise from the vacuum at frequencies ω and ω' is dominating if compared to the leading-order solution. This means that only small values of squeezing are consistent with the perturbative approach.

V. PHOTON MULTIPLICATION AND MULTI-PHOTON ABSORPTION

In this section, we analyze how individual single- and multi-photon states scatter at a DC-voltage biased Josephson junction. Rather than evaluating temporal changes in the photon flux density due to Fock-state pulses, a more informative approach here is the evaluation of the scattering amplitudes of type

$$T^{1 \rightarrow n} = T(\omega \rightarrow \omega_1 \dots \omega_n) \quad (67)$$

$$= \left\langle [\hat{a}_{\text{out}}(\omega_1) \dots \hat{a}_{\text{out}}(\omega_n)] \hat{a}_{\text{in}}^\dagger(\omega) \right\rangle. \quad (68)$$

The ensemble average is made with respect to vacuum state, which we mark as $|0\rangle$. This gives the amplitude for that single incoming photon of frequency ω converts into n outgoing photons of frequencies $\omega_1, \dots, \omega_n$. The total amplitude for an incoming wavepacket is then an integration over individual frequencies with corresponding amplitudes: integration over $\xi(\omega)$ as in Eq. (15). The total outgoing state includes integration over all frequencies $\omega_1, \dots, \omega_n$. Similarly for multi-photon inputs.

It should be now noted that results for coherent and thermal inputs, presented in Sec. III, can in principle be derived by combining this scattering-matrix approach with proper statistical average over incoming multi-photon states. We also note that in this article we do a leading-order perturbation theory in powers of E_J and that this approach is also valid for more general electromagnetic environments. An exact solution in powers of E_J using a narrow bandwidth approximation, i.e., in the case of sharp resonances in the environment, has been derived in Ref. [39].

A. Output expressed using a continuous-mode displacement operator

We start by making a useful and interesting connection between the leading-order solution for the outgoing field and a continuous-mode displacement operator. This connection, and mathematical properties that follow, directly imply the form of the scattering elements between arbitrary photon-number states.

For this we write the (zeroth-order) phase difference at the junction, Eq. (20), in the form

$$\begin{aligned} i\hat{\phi}_0(t) &= i \frac{\sqrt{4\pi\hbar Z_0}}{\Phi_0} \int_0^\infty \frac{d\omega}{\sqrt{\omega}} A(\omega) \hat{a}_{\text{in}}(\omega) e^{-i\omega t} - \text{H.c.} \\ &\equiv \hat{a}_\alpha - \hat{a}_\alpha^\dagger. \end{aligned} \quad (69)$$

Here, we have defined an unnormalized photon creation

operator

$$\hat{a}_\alpha^\dagger = \int_0^\infty d\omega \alpha(\omega) e^{i\omega t} \hat{a}_{\text{in}}^\dagger(\omega) \quad (70)$$

$$\alpha(\omega) = -\frac{i}{\Phi_0} \sqrt{\frac{4\pi\hbar Z_0}{\omega}} A^*(\omega) = -i \sqrt{\frac{2Z_0}{R_Q \omega}} A^*(\omega) \quad (71)$$

For simplicity, we now neglect backward Cooper-pair tunneling, i.e., the term $\propto e^{i(\omega+\omega_J)t}$ in the leading-order solution of operator $\hat{a}_{\text{out}}(\omega)$. By using the definitions of Eqs. (69-71), we can then express the perturbative solution as

$$\begin{aligned} \hat{a}_{\text{out}}(\omega) &= -\frac{\alpha^*(\omega)}{\alpha(\omega)} \hat{a}_{\text{in}}(\omega) \\ &+ \frac{I_c}{4e} \alpha^*(\omega) \int_{-\infty}^\infty dt e^{i(\omega-\omega_J)t} \exp[\hat{a}_\alpha - \hat{a}_\alpha^\dagger]. \end{aligned} \quad (72)$$

The out-field annihilation operator is now defined in terms of a continuous-mode displacement operator

$$\exp[\hat{a}_\alpha - \hat{a}_\alpha^\dagger] \equiv \hat{D}^\dagger(\alpha). \quad (73)$$

This connection originates from the form of the Josephson Hamiltonian ($\cos \hat{\phi}$ term), which in the quantized theory makes discrete shifts to the junction charge (Cooper-pair tunneling).

We can now exploit the following important properties of a continuous-mode coherent state [40]

$$|\alpha(\omega)\rangle \equiv \hat{D}(\alpha)|0\rangle = \exp[\hat{a}_\alpha^\dagger - \hat{a}_\alpha] |0\rangle, \quad (74)$$

for which applies

$$\hat{a}_{\text{in}}(\omega)|\alpha(\omega)\rangle = \alpha(\omega) e^{i\omega t} |\alpha(\omega)\rangle \quad (75)$$

$$\langle 0|\alpha(\omega)\rangle = \exp\left[-\int d\omega |\alpha(\omega)|^2/2\right]. \quad (76)$$

The operator $\hat{D}(\alpha)$ satisfies

$$[\hat{a}_{\text{in}}(\omega), \hat{D}^{(\dagger)}(\alpha)] = (-)\alpha(\omega) e^{i\omega t} \hat{D}^{(\dagger)}(\alpha). \quad (77)$$

B. Evaluation of the scattering matrix

Using the connection to the continuous-mode displacement operator, it is straightforward to evaluate general multi-photon scattering amplitudes to the leading order of I_c . We then write the general result in the form

$$T^{m \rightarrow n} = T_0^{m \rightarrow n} + T_1^{m \rightarrow n} + \dots \quad (78)$$

according to the order in the critical current.

1. Single-photon processes

Let us first consider the zeroth order contribution T_0 . Using Eq. (72), we get (using $I_c = 0$)

$$\begin{aligned} T_0^{1 \rightarrow 1} &= \langle \hat{a}_{\text{out}}(\omega_1) \hat{a}_{\text{in}}^\dagger(\omega) \rangle_0 = -\frac{\alpha^*(\omega_1)}{\alpha(\omega_1)} \langle \hat{a}_{\text{in}}(\omega_1) \hat{a}_{\text{in}}^\dagger(\omega) \rangle \\ &= -\frac{\alpha^*(\omega_1)}{\alpha(\omega_1)} \delta(\omega - \omega_1). \end{aligned} \quad (79)$$

Here we used the relation $[\hat{a}_{\text{in}}(\omega), \hat{a}_{\text{in}}^\dagger(\omega')] = \delta(\omega - \omega')$ and that $\hat{a}_{\text{in}}|0\rangle = 0$. This element describes elastic scattering of an incoming photon. Such contribution exists only in the scattering between single-photon states, i.e., $T_0^{1 \rightarrow n} = 0$ for $n > 1$.

The leading order correction to the single-photon scattering is obtained by using the term proportional to I_c in the out field,

$$\begin{aligned} T_1^{1 \rightarrow 1} &= \langle \hat{a}_{\text{out}}(\omega_1) \hat{a}_{\text{in}}^\dagger(\omega) \rangle_1 \\ &= \frac{I_c}{4e} \int_{-\infty}^{\infty} dt e^{i(\omega_1 - \omega_J)t} \alpha^*(\omega_1) \langle \hat{D}^\dagger(\alpha) \hat{a}_{\text{in}}^\dagger(\omega) \rangle \\ &= \frac{I_c}{4e} e^{-\tilde{\rho}/2} \alpha^*(\omega) \alpha^*(\omega_1) 2\pi \delta(\omega_J + \omega - \omega_1), \end{aligned} \quad (80)$$

where we have used Eq. (75). This describes inelastic scattering of an incoming photon, where the electrostatic energy released in a Cooper-pair tunneling is absorbed, $\omega_1 = \omega + \omega_J$. The appearance of parameter

$$\tilde{\rho} \equiv \int_0^\infty |\alpha(\omega)|^2 d\omega = \int_0^\infty \frac{d\omega}{\omega} \frac{2\text{Re}[Z_t(\omega)]}{R_Q} \quad (81)$$

follows from Eq. (76). The expression as a function of tunnel impedance follows from Eqs. (71) and (27).

The parameter $\tilde{\rho}$ corresponds to the average photon number of a coherent state $|\alpha(\omega)\rangle$,

$$\tilde{\rho} = \langle \alpha(\omega) | \int d\omega' \hat{a}^\dagger(\omega') \hat{a}(\omega') | \alpha(\omega) \rangle \quad (82)$$

From Eq. (81) we find that in the case of a finite density of states at $\omega = 0$ we have $\tilde{\rho} \rightarrow \infty$ and consequently the tunneling elements go to zero. This manifests dephasing due to low-frequency noise. As this is a zero-frequency effect, the amplitudes do have finite momentary values, but vanishing long-time averages. It can also be shown that the factor $\exp(-\tilde{\rho})$ is a continuous-mode generalization of the renormalization factor $\exp(-\rho)$ in the $P(E)$ -function of single-mode environment [2].

2. Multi-photon processes

Let us consider now multi-photon production, i.e., the case $n \geq 2$ in Eq. (67). To evaluate this in the first order of I_c , we insert the displacement operator once in the n

possible out-operators in expression

$$T^{1 \rightarrow n} = \langle [\hat{a}_{\text{out}}(\omega_1) \dots \hat{a}_{\text{out}}(\omega_n)] \hat{a}_{\text{in}}^\dagger(\omega) \rangle.$$

We find that the result is non-zero only if the leading-order solution for the out-field is inserted to operators of frequencies ω_{n-1} or ω_n . We now write the leading-order result in the form

$$T_1^{1 \rightarrow n} = \mathcal{T}^{1 \rightarrow n} + \sum_{i=1}^n t_i^{1 \rightarrow n}, \quad (83)$$

where the first part has the form

$$\begin{aligned} \mathcal{T}^{1 \rightarrow n} &= \frac{I_c}{2e} \pi e^{-\tilde{\rho}/2} \delta(\omega + \omega_J - \omega_1 - \dots - \omega_n) \\ &\times \alpha^*(\omega) \alpha^*(\omega_1) \dots \alpha^*(\omega_n), \end{aligned} \quad (84)$$

which describes n -photon emission with energy conservation, $\omega + \omega_J = \omega_1 + \dots + \omega_n$. We also get n additional terms of the form

$$\begin{aligned} t_1^{1 \rightarrow n} &= \frac{I_c}{2e} \pi e^{-\tilde{\rho}/2} \delta(\omega - \omega_1) \delta(\omega_J - \omega_2 - \omega_3 - \dots - \omega_n) \\ &\times \frac{\alpha^*(\omega_1)}{\alpha(\omega_1)} \alpha^*(\omega_2) \alpha^*(\omega_3) \dots \alpha^*(\omega_n). \end{aligned} \quad (85)$$

Such terms manifest an elastic reflection of the input photon of frequency ω to mode ω_i : The rest of the observations are due to direct emission (without input). We then find that a multiphoton state in the output is possible even when the incoming photon is scattered elastically, since a DC-voltage-biased Josephson junction emits radiation also without input. If the additional emission is unwanted, it can be reduced by engineering the tunnel impedance, $\text{Re}[Z_t(\omega)] = Z_0 |A(\omega)|^2 \propto |\alpha(\omega)|^2$, so that it vanishes or has a small value at frequencies that need to be populated in unwanted processes [39].

Consider then scattering amplitudes between general photon-number states. Assuming an m -photon input, we get for the term describing the full conversion to n -photon output (no elastic reflections),

$$\begin{aligned} \mathcal{T}^{m \rightarrow n} &= \frac{I_c}{2e} \pi e^{-\tilde{\rho}/2} \\ &\times \alpha^*(\omega'_1) \dots \alpha^*(\omega'_m) \alpha^*(\omega_1) \dots \alpha^*(\omega_n) \\ &\times \delta(\omega'_1 + \dots + \omega'_m + \omega_J - \omega_1 - \dots - \omega_n), \end{aligned} \quad (86)$$

where the incoming frequencies are now labeled as $\omega'_1 \dots \omega'_m$. Rest of obtained terms (not shown) describe full conversion of only part of the incoming photons, similarly as above in the case of single-photon input.

We then obtain that an incoming single photon can create any n -photon state in the output, or vice versa, any n -photon state in the input can get converted to a single-photon output. The first process corresponds to photon multiplication and the latter one to non-linear dissipation. The corresponding amplitudes are described

by the function $\alpha(\omega)$, Eq. (71), which can be tailored to support only desired processes. It should also be emphasized that such states can violate the Bell inequalities for energy and time [39, 53] and the considered system can thereby be useful for quantum-information applications.

VI. CONCLUSIONS AND DISCUSSION

In conclusion, we have analyzed how incoming microwaves of different forms scatter by a DC-voltage biased Josephson junction. Scattering effects for general circuits were described in terms of $P(E)$ function and expectation values of a displacement operator. The main practical findings were that thermal and coherent radiation can be absorbed and amplified in a circuit with a resonance frequency, and that coherent radiation can be converted into two-mode squeezed microwaves, observable mainly at overbias frequencies. Furthermore, the non-linear interaction at the junction allows for engineering, in principle, any photon multiplication and multiphoton absorption processes, with appropriate tailoring of the impedance seen by the Josephson junction. The considered circuits then offer new ways to process quantum microwaves on-chip, experimentally demonstrated examples including quantum-limited amplification [20], microwave lasing [18], and microsecond calorimetry [15].

The analysis presented in this article was made in the perturbative regime, which is very useful for understanding inelastic Cooper-pair tunneling in general electromag-

netic environments. In the strict validity region of the perturbative solution, the incoming radiation is mostly reflected, rather than scattered to different modes. However, it should be emphasized that theories applicable in the opposite limits, for example, with sharply peaked environmental impedance, can be straightforwardly established for desired situations [26, 27, 39]. Also non-perturbative methods through self-consistent expansions [43] or direct evaluation of relevant higher-order contributions [22, 24] are possible.

A great future theoretical interest is a deeper understanding of quantum information created by quantum transport, and its accurate engineering by microwave circuit design. In particular, the created radiation can be made to consist of high-photon-number bundles and show very strong bunching. It can also carry information of the underlying quantum transport in various forms. The radiation can also be tailored to be broadband and bright, or concentrated to certain resonance frequencies. New methods and ideas for characterization and detection of created and carried quantum information in such forms of microwave light are then desired theoretically and experimentally.

Acknowledgments

The authors thank M. Hofheinz, F. Portier, D. Hazra, S. Jebari, and G. Johansson for fruitful discussions. This work was supported by the DFG Grant No. MA 6334/3-1.

-
- [1] M. H. Devoret, D. Esteve, H. Grabert, G.-L. Ingold, H. Pothier, and C. Urbina, Phys. Rev. Lett. **64**, 1824 (1990).
 - [2] G.-L. Ingold and Yu. V. Nazarov, in *Single Charge Tunneling: Coulomb Blockade Phenomena in Nanostructures*, edited by H. Grabert and M. H. Devoret (Plenum, New York, 1992), p.21.
 - [3] T. Holst, D. Esteve, C. Urbina, and M. H. Devoret, Phys. Rev. Lett. **73**, 3455 (1994).
 - [4] J. Leppäkangas, E. Thuneberg, R. Lindell, and P. Hakonen, Phys. Rev. B **74** 054504 (2006).
 - [5] Yu. A. Pashkin, H. Im, J. Leppäkangas, T. F. Li, O. Astafiev, A. A. Abdumalikov Jr., E. Thuneberg, and J. S. Tsai, Phys. Rev. B **83**, 020502(R) (2011).
 - [6] A. Cottet, T. Kontos, and B. Doucot, Phys. Rev. B **91**, 205417 (2015).
 - [7] C. Altimiras, F. Portier, and P. Joyez, Phys. Rev. X **6**, 031002 (2016).
 - [8] M. Hofheinz, F. Portier, Q. Baudouin, P. Joyez, D. Vion, P. Bertet, P. Roche, and D. Esteve, Phys. Rev. Lett. **106**, 217005 (2011).
 - [9] G. Gasse, C. Lupien, and B. Reulet, Phys. Rev. Lett. **111**, 136601 (2013).
 - [10] J.-C. Forgues, C. Lupien, and B. Reulet, Phys. Rev. Lett. **113**, 043602 (2014).
 - [11] J.-C. Forgues, C. Lupien, and B. Reulet, Phys. Rev. Lett. **114**, 130403 (2015).
 - [12] C. Altimiras, O. Parlavacchio, P. Joyez, D. Vion, P. Roche, D. Esteve, and F. Portier, Phys. Rev. Lett. **112**, 236803 (2014).
 - [13] F. Chen, J. Li, A. D. Armour, E. Brahim, J. Stettenheim, A. J. Sirois, R. W. Simmonds, M. P. Blencowe, and A. J. Rimberg Phys. Rev. B **90**, 020506(R) (2014).
 - [14] Y.-Y. Liu, J. Stehlik, C. Eichler, M. J. Gullans, J. M. Taylor, and J. R. Petta, Science **347**, 285 (2015).
 - [15] O.-P. Saira, M. Zgirski, K. L. Viitanen, D. S. Golubev, J. P. Pekola, Phys. Rev. Applied **6**, 024005 (2016).
 - [16] S. Masuda, K. Y. Tan, M. Partanen, R. E. Lake, J. Govenius, M. Silveri, H. Grabert, M. Möttönen, arXiv:1612.06822.
 - [17] J. Sarkar, C. Padurariu, A. Puska, D. Golubev, and P. J. Hakonen, arXiv:1706.02895.
 - [18] M. C. Cassidy, A. Bruno, S. Rubbert, M. Irfan, J. Kammhuber, R. N. Schouten, A. R. Akhmerov, and L. P. Kouwenhoven, Science **355**, 939 (2017).
 - [19] M. Westig, B. Kubala, O. Parlavacchio, Y. Mukharsky, C. Altimiras, P. Joyez, D. Vion, P. Roche, M. Hofheinz, D. Esteve, M. Trif, P. Simon, J. Ankerhold, and F. Portier, Phys. Rev. Lett. **119**, 137001 (2017).
 - [20] S. Jebari, F. Blanchet, A. Grimm, D. Hazra, R. Albert, P. Joyez, D. Vion, D. Esteve, F. Portier, and M. Hofheinz, arXiv:1704.04432.

- [21] F. Hassler and D. Otten, Phys. Rev. B **92**, 195417 (2015).
- [22] F. Xu, C. Holmqvist, and W. Belzig, Phys. Rev. Lett. **113**, 066801 (2014).
- [23] F. Qassemi, A. L. Grimsmo, B. Reulet, and A. Blais, Phys. Rev. Lett. **116**, 043602 (2016).
- [24] J. Leppäkangas, M. Fogelström, M. Marthaler, and G. Johansson, Phys. Rev. B (2016).
- [25] J. Leppäkangas, G. Johansson, M. Marthaler, and M. Fogelström, Phys. Rev. Lett. **110**, 267004 (2013).
- [26] A. D. Armour, M. P. Blencowe, E. Bahimi, A. J. Rimberg, Phys. Rev. Lett. **111** 247001 (2013).
- [27] V. Gramich, B. Kubala, S. Rocher, J. Ankerhold, Phys. Rev. Lett. **111** 247002 (2013).
- [28] N. Lambert, F. Nori, and C. Flindt, Phys. Rev. Lett. **115** 216803 (2015).
- [29] M. Marthaler, J. Leppäkangas, and J. H. Cole, Phys. Rev. B **83**, 180505(R) (2011).
- [30] S. Dambach, B. Kubala, V. Gramich, and J. Ankerhold, Phys. Rev. B **92**, 054508 (2015).
- [31] J.-R. Souquet and A. A. Clerk, Phys. Rev. A **93**, 060301(R) (2016).
- [32] J. Leppäkangas, M. Fogelström, A. Grimm, M. Hofheinz, M. Marthaler, and G. Johansson, Phys. Rev. Lett. **115** 027004 (2015).
- [33] C. W. J. Beenakker and H. Schomerus, Phys. Rev. Lett. **86** 700 (2001).
- [34] J. Leppäkangas, G. Johansson, M. Marthaler, and M. Fogelström, New J. Phys. **16**, 015015 (2014).
- [35] M. Trif and P. Simon, Phys. Rev. B **92**, 014503 (2015).
- [36] C. Mora, C. Altimiras, P. Joyez, and F. Portier, Phys. Rev. B **95**, 125311 (2017).
- [37] U. C. Mendes and C. Mora, New J. Phys. **17**, 113014 (2015).
- [38] U. C. Mendes, P. Joyez, B. Reulet, A. Blais, F. Portier, C. Mora, C. Altimiras, arXiv:1802.07323.
- [39] J. Leppäkangas, M. Marthaler, D. Hazra, S. Jebari, R. Albert, F. Blanchet, G. Johansson, and M. Hofheinz, Phys. Rev. A **97**, 013855 (2018).
- [40] R. Loudon, *The Quantum Theory of Light* (Oxford University, New York, 2010).
- [41] C. Gardiner and P. Zoller, *Quantum Noise* (Springer, Berlin, 2004).
- [42] H. Grabert, G.-L. Ingold, and B. Paul, Europhys. Lett. **44**, 360 (1998).
- [43] M. Marthaler and J. Leppäkangas, Phys. Rev. B **94**, 144301 (2016).
- [44] M. Frey and H. Grabert, Phys. Rev. B **94**, 045429 (2016).
- [45] D. F. Walls and G.J. Milburn, *Quantum Optics* (Springer, Berlin, 2008).
- [46] J. R. Johansson, G. Johansson, C. M. Wilson, P. Delsing, and F. Nori, Phys. Rev. A **87**, 043804 (2013).
- [47] C. M. Wilson, G. Johansson, A. Pourkabirian, M. Simoen, J. R. Johansson, T. Duty, F. Nori, and P. Delsing, Nature **479**, 376 (2011).
- [48] C. Eichler, C. Lang, J. M. Fink, J. Govenius, S. Filipp, and A. Wallraff, Phys. Rev. Lett. **109**, 240501 (2012).
- [49] P. Lähteenmäki, G. S. Paraoanu, J. Hassel, and P. J. Hakonen, Proc. Natl. Acad. Sci. U.S.A **110**, 4234 (2013).
- [50] P. D. Nation, J.R. Johansson, M. P. Blencowe, and F. Nori, Rev. Mod. Phys. **84**, 1 (2012).
- [51] B. H. Schneider, A. Bengtsson, I. M. Svensson, T. Aref, G. Johansson, J. Bylander, and P. Delsing, arXiv:1802.05529.
- [52] A. Miranowicz, M. Bartkowiak, X. Wang, Y. Liu, and F. Nori, Phys. Rev. A **82**, 013824 (2010).
- [53] J. D. Franson, Phys. Rev. Lett. **62**, 2205 (1989).

Appendix A: Calculation of the photon flux density

The evaluation of quantities such as the emission spectrum is done similarly as presented in Refs. [25,34,32,24]. These works consider a thermal input but in the absence of coherent incoming radiation. The difference that appears is induced sidebands. Also here, 'non-diagonal' contributions in the photon flux density play a more central role, as discussed below.

Consider first the evaluation of 'diagonal' contribution $f_{11}(\omega) \equiv \int_0^\infty d\omega' \langle \hat{a}_1^\dagger(\omega) \hat{a}_1(\omega') \rangle$ for general input fields. The leading-order solution for the out-field operator $\hat{a}_{\text{out}}(\omega)$ to be used here is

$$\begin{aligned} \hat{a}_1(\omega) &= iI_c \sqrt{\frac{Z_0}{\hbar\omega\pi}} A(\omega) \int_{-\infty}^{\infty} dt e^{i\omega t} \sin[\omega_J t + a \cos \omega_0 t - \hat{\phi}_0(t)] \\ &= iI_c \sqrt{\frac{Z_0}{\hbar\omega\pi}} A(\omega) \int_{-\infty}^{\infty} dt e^{i\omega t} \left[\frac{1}{2i} e^{i\omega_J t - i\hat{\phi}_0(t)} \sum_{n=-\infty}^{\infty} i^n J_n(a) e^{in\omega_0 t} + \text{H.c.} \right]. \end{aligned}$$

Here we have used

$$e^{ia \cos \omega_0 t} = \sum_{n=-\infty}^{\infty} i^n J_n(a) e^{in\omega_0 t}.$$

We get for forward directed tunneling

$$\begin{aligned} \langle \hat{a}_1^\dagger(\omega) \hat{a}_1(\omega') \rangle &= \int_{-\infty}^{\infty} dt \int_{-\infty}^{\infty} dt' e^{-i(\omega - \omega_J)t + i(\omega' - \omega_J)t'} \times \\ &\times (i)^n (-i)^m \sum_{n=-\infty}^{\infty} \sum_{m=-\infty}^{\infty} e^{-im\omega_0 t'} e^{in\omega_0 t} \langle e^{-i\hat{\phi}_0(t)} e^{i\hat{\phi}_0(t')} \rangle J_m(a) J_n(a). \end{aligned}$$

We do a change of integration variables

$$\begin{aligned} x &= t - t' & t &= \frac{x}{2} + y \\ y &= \frac{t + t'}{2} & t' &= y - \frac{x}{2} \end{aligned}$$

Integration over the variable y leads to the relevant energy factor

$$2\pi\delta[\omega - \omega' - (n - m)\omega_0] e^{ix(\omega_J - \omega + n\omega_0)}. \quad (\text{A1})$$

Assuming $n = m$ leads to (including both tunneling directions)

$$\langle \hat{a}_1^\dagger(\omega) \hat{a}_1(\omega') \rangle = \sum_{\pm} \sum_{n=-\infty}^{\infty} \frac{\pi I_c^2 Z_0 |A(\omega)|^2}{\omega} P[\hbar(\pm\omega_J + n\omega_0 - \omega)] |J_n(a)|^2 \delta(\omega - \omega'). \quad (\text{A2})$$

It should be noted that there are also nondiagonal terms in frequency (for which $\omega \neq \omega'$), differing by multiples of ω_0 . These terms describe a beating effect in $f(\omega) = \int d\omega' \langle \hat{a}^\dagger(\omega) a(\omega') \rangle / 2\pi$, due to interference between different (coherent) frequencies in the output, but do not contribute to time averages, where only the contribution of Eq. (A2) remains. Nondiagonal terms in this correlator have generally the form

$$\langle \hat{a}_1^\dagger(\omega) a_1(\omega') \rangle = \sum_{n,m=-\infty}^{\infty} \frac{\pi I_c^2 Z_0 A^*(\omega) A(\omega')}{\sqrt{\omega\omega'}} P[\hbar(\omega_J + n\omega_0 - \omega)] J_n(a) J_m(a) (i)^n (-i)^m \delta[\omega - \omega' - (n - m)\omega_0].$$

In the case of squeezing analysis, we assume $\omega, \omega' < \omega_0$, which means that these terms do not contribute there either. However, analogous terms do contribute in the time averages of the squeezing operator, $\langle a_1(\omega) a_1(\omega') \rangle$, as shown below.

The additional 'non-diagonal' contribution $\langle \hat{a}_2^\dagger(\omega) \hat{a}_0(\omega') \rangle + \langle \hat{a}_0^\dagger(\omega) \hat{a}_2(\omega') \rangle$ has been evaluated in Ref. [34] for the case $a = 0$. For finite a they produce additional delta-function terms to frequency ω_0 . The direct evaluation is somewhat cumbersome for general a but the result is phenomenologically clear. We confirm that the given formulas are correct by energy-conservation analysis, shown below.

Appendix B: Energy conservation

The given formulas describe microwave conversion between different frequencies, mediated by Cooper-pair tunneling. It is clear that for a consistent description, the energy conservation is crucial. To show this, we need to compare the power of the propagating electromagnetic radiation to the energy provided by the voltage source, IV . All quantities have to be calculated to up to the same order in the tunneling coupling. We can prove the energy conservation straightforwardly for a thermal input and weak coherent drive $a < 1$, whereas for larger a the energy conservation was taken as a starting point to verify that the introduced expression for absorption and emission at the drive mode are consistent.

Let us now consider energy conservation in the presented theory. The key to the proof is the relation (considering first the case of thermal input)

$$\begin{aligned} \frac{d}{dt} \exp[J(t)] &= -i \exp[J(t)] \int_0^\infty d\omega \frac{Z_0 |A(\omega)|^2}{R_Q} \times \\ &\left[\left(1 + \coth\left(\frac{1}{2}\beta\hbar\omega\right) \right) e^{-i\omega t} + \left(1 - \coth\left(\frac{1}{2}\beta\hbar\omega\right) \right) e^{i\omega t} \right]. \end{aligned}$$

By Fourier transforming one obtains

$$EP(E) = \int_0^\infty \hbar d\omega \frac{Z_0 |A(\omega)|^2}{R_Q} P(E - \hbar\omega) \left[1 + \coth\left(\frac{1}{2}\beta\hbar\omega\right) \right] \\ + \int_0^\infty \hbar d\omega \frac{Z_0 |A(\omega)|^2}{R_Q} P(E + \hbar\omega) \left[1 - \coth\left(\frac{1}{2}\beta\hbar\omega\right) \right]$$

By identifying $E = 2eV$ and using the leading-order result for the forward Cooper-pair tunneling,

$$I^\pm = \frac{\pi \hbar I_c^2}{4e} P(\pm 2eV), \quad (\text{B1})$$

the work done by the voltage source gets related to the power spectral density,

$$I^+ V = \frac{I_c^2}{4} \int_0^\infty \hbar d\omega Z_0 |A(\omega)|^2 P(2eV - \hbar\omega) \left[1 + \coth\left(\frac{1}{2}\beta\hbar\omega\right) \right] \\ + \frac{I_c^2}{4} \int_0^\infty \hbar d\omega Z_0 |A(\omega)|^2 P(2eV + \hbar\omega) \left[1 - \coth\left(\frac{1}{2}\beta\hbar\omega\right) \right]. \quad (\text{B2})$$

The contribution from the backward tunneling is obtained by changing $V \rightarrow -V$. Now it can be shown that

$$(I^+ - I^-)V = \int_0^\infty d\omega \hbar\omega [f_{\text{em}}(\omega) - f_{\text{abs}}(\omega)]. \quad (\text{B3})$$

This states that the extra power in the output is the same as the work done by the external voltage source.

For a coherent state with a dimensionless amplitude a one can proceed similarly. There are now two types of contributions in the photon spectrum $f_{\text{em}}(\omega) - f_{\text{abs}}(\omega)$: (i) terms as before but with shifted energy arguments (when $n \neq 0$) and front factors $|J_n|^2$, and (ii) terms proportional to delta functions at the drive frequency ω_0 . The junction current I has only contributions that are similar to terms (i).

Consider now obtaining the total power, $\int d\omega [f_{\text{em}}(\omega) - f_{\text{abs}}(\omega)]$, term by term from the equation for the current, Eq. (B2). The case $n = 0$ comes out by multiplying both sides of Eq. (B2) by a front factor $|J_0|^2$. The case $n \neq 0$ needs multiplying both sides by $|J_n|^2$ and changing the energy argument as $E \rightarrow E + n\hbar\omega_0$ and thereby $V \rightarrow V + n\hbar\omega_0/2e$. The term proportional to V then corresponds to the terms (i) in the radiation spectrum. Additional contributions proportional to $n\omega_0 P(E + n\omega_0) |J_n|^2$ correspond to terms (ii), with a sign difference. Moving the additional terms of type (ii) to the other side gives us the relation

$$(I^+ - I^-)V = \int_0^\infty d\omega \hbar\omega [f_{\text{em}}(\omega) - f_{\text{abs}}(\omega)]. \quad (\text{B4})$$

The given equations then satisfy energy conservation also for the case of incoming coherent state ($a \neq 0$).

Appendix C: Calculation of the squeezing correlator

In the presence of a coherent input field, effects that are phase sensitive can prevail. We evaluate here the correlator $\langle \hat{a}_{\text{out}}(\omega) \hat{a}_{\text{out}}(\omega') \rangle$ between frequencies that sum to the drive frequency, $\omega + \omega' = \omega_0$. It is only the expectation value $\langle \hat{a}_1(\omega) \hat{a}_1(\omega') \rangle$ that gives a finite contribution when $\omega, \omega' \neq \omega_0$ and $\omega, \omega' \gg k_b T / \hbar$.

We get two contributions for this correlator (neglecting an additional front factor $-I_c^2 Z_0 A(\omega) A(\omega') / 4\sqrt{\omega\omega'} \hbar\pi$)

$$\int_{-\infty}^\infty dt \int_{-\infty}^\infty dt' e^{i\omega t + i\omega' t' + i\omega_J(t-t')} e^{J(t-t')} \sum_{n=-\infty}^\infty \sum_{m=-\infty}^\infty (i)^n (-i)^m e^{in\omega_0 t} e^{-im\omega_0 t'} J_n(a) J_m(a),$$

and

$$\int_{-\infty}^\infty dt \int_{-\infty}^\infty dt' e^{i\omega t + i\omega' t' - i\omega_J(t-t')} e^{J(t-t')} \sum_{n=-\infty}^\infty \sum_{m=-\infty}^\infty (-i)^n (i)^m e^{-in\omega_0 t} e^{im\omega_0 t'} J_n(a) J_m(a).$$

We do the same change of integration variables as in Appendix A, integrate over y , and obtain the energy factor of

the first term

$$2\pi\delta[\omega + \omega' + (n - m)\omega_0]e^{i(\omega + \omega_J + n\omega_0)} \quad (\text{C1})$$

The energy factor of the second term has the form

$$2\pi\delta[\omega + \omega' - (n - m)\omega_0]e^{ix(\omega - \omega_J - n\omega_0)}, \quad (\text{C2})$$

Assuming $\omega + \omega' = \omega_0$ leads to conditions $n - m = -1$ (first contribution) and $n - m = 1$ (second contribution).

Accounting for $\int_{-\infty}^{\infty} dx e^{J(x) + iE/\hbar} = 2\pi\hbar P(E)$, the explicit result is then

$$\begin{aligned} \langle \hat{a}_1(\omega) \hat{a}_1(\omega') \rangle = & - i4\pi^2 \hbar \delta(\omega + \omega' - \omega_0) \sum_{n=-\infty}^{\infty} P[\hbar(\omega + \omega_J + n\omega_0)] J_n(a) J_{n+1}(a) \\ & - i4\pi^2 \hbar \delta(\omega + \omega' - \omega_0) \sum_{n=-\infty}^{\infty} P[\hbar(\omega - \omega_J - n\omega_0)] J_n(a) J_{n-1}(a). \end{aligned} \quad (\text{C3})$$

Noting that for odd values of n we have $J_{-n}(a) = -J_n(a)$ and for even values $J_{-n}(a) = J_n(a)$, this can be rewritten as

$$\langle \hat{a}_1(\omega) \hat{a}_1(\omega') \rangle = \sum_{\pm} \mp i4\pi^2 \hbar \delta(\omega + \omega' - \omega_0) \sum_{n=-\infty}^{\infty} P[\hbar(\omega \pm \omega_J + n\omega_0)] J_n(a) J_{n+1}(a). \quad (\text{C4})$$